

Numerical simulations of the plasma-wall transition in a weakly collisional and magnetized plasma

S.Devaux¹, G.Manfredi²

¹ LPMIA, UMR 7040 UHP Nancy I - CNRS

BP 239 54506 Vandoeuvre-lès-Nancy Cedex, France

² Institut de Physique et Chimie des Matériaux de Strasbourg

UMR 7504 ULP-CNRS, 23 rue du Loess, BP 43, 67034 Strasbourg Cedex 2, France

Introduction

The plasma-wall transition problem is present in the large majority of research fields in plasma physics. In magnetically confined fusion devices, knowledge of the particles characteristics in the plasma edge is very important. Indeed, these particles can erode the wall, thus reducing the lifetime of the components facing the plasma. In addition, energetic particles hitting the wall may deteriorate the quality of the plasma confinement, because high-Z impurity particles are released from the wall and pollute the plasma. In low temperature plasmas, plasma-wall interactions are even more fundamental, because treating a surface is often the very goal to achieve. Plasma-wall interactions are also crucial to interpret probe measurements, as the interaction of the plasma with the probe surface can substantially alter the outcome of the measurement [1]. Here, we present results obtained from numerical simulations of the interaction between a semi-infinite wall and a weakly collisional argon plasma, when a tilted magnetic field is applied. The use of a Vlasov code [2] allows us to resolve the various regions of the transition layer with great accuracy.

Model and numerical methods

The kinetic numerical methods employed here are based on the distribution function $f(x, v)$, which represents the particle probability density in phase space. This function can be used to compute standard macroscopic quantities such as the particle density $n = \int f dv$ or the average fluid velocity $\vec{u} = \int f \vec{v} dv / n$. The evolution of the distribution function is governed by the self-consistent Vlasov-Poisson system, with Maxwell-distributed electrons:

$$\frac{\partial f_i}{\partial t} + v_x \frac{\partial f_i}{\partial x} - \frac{e}{m} \left(\frac{\partial \phi}{\partial x} - \vec{v} \times \vec{B} \right) \frac{\partial f_i}{\partial \vec{v}} = 0 \quad (1)$$

$$\frac{\partial^2 \phi}{\partial x^2} = -\frac{e}{\epsilon_0} \left(\int f_i dv - n_e(\phi) \right) \quad (2)$$

$$n_e(\phi) = n_0 \exp(e\phi / k_B T_e) \quad (3)$$

Here subscript i refers to ions and subscript e to electrons; e is the absolute electron charge, ϕ the self-consistent electric potential, and ϵ_0 the vacuum dielectric permittivity. The model (1)-(3) does not take into account collisional effects. Typical values of mean free paths in low-pressure plasma devices are 104cm and 106cm, respectively, for ion-ion and ion-electron collisions, and are much larger than the typical size of the device (≈ 100 cm). These collisions can thus be neglected. On the other hand, the ion-neutral mean free path is of order 10cm, and this effect has to be taken into account. Here, we will use a simple relaxation model, which reflects the fact that collisions tend to reconstruct the equilibrium Maxwellian distribution $f_0(v)$:

$$\left(\frac{\partial f_i}{\partial t}\right)_{\text{coll}} = -\nu(f_i - f_0) \tag{4}$$

where ν represents the collision frequency. The Vlasov equation is solved with an Eulerian code based on a fixed mesh covering the entire phase-space. Unlike in Particle-In-Cell (PIC) codes, the ion distribution function is defined as a smooth function of the phase space variables. The time integration relies on a splitting scheme, which treats each phase space direction separately. This approach has the advantage of reducing the numerical noise compared to PIC simulations.

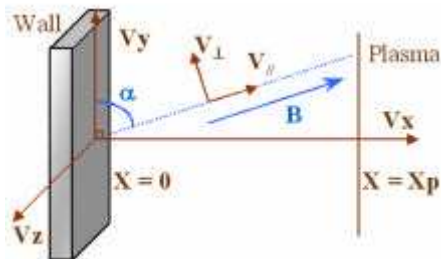


Figure 1: Plasma-wall transition

Here, we consider the interaction between an unmagnetized plasma, located at $x \geq x_p$ and an infinite wall. We assume the wall to be perfectly absorbant, i.e. all particles hitting the wall are lost. The tilted magnetic field lies in the xOy plane, and make an angle α with the Oy direction. Due to the planar symmetry, the phase space can be reduced to one dimension in space and three dimensions in velocity, as shown in Fig.1. The initial condition corresponds to a plasma at thermodynamic equilibrium, with a Maxwellian distribution at temperature T_0 . The results

presented in the forthcoming sections always refer to asymptotic steady state configurations, obtained by running the code for a sufficiently long time.

Numerical results

In the special case of a "medium" strength of the magnetic field, characterized by

$$\lambda_{De} \ll r_{Li} \ll \lambda_{mfp}, \tag{5}$$

where λ_{De} is the Debye length, r_{Li} is the ion Larmor radius and λ_{mfp} is the ion-neutral mean-free-path, the transition is divided into three different regions [3, 4], as shown in Fig. 2, where the velocity distribution in the $v_x - v_y$ plane is plotted. Fig.2a is located in the bulk plasma, the

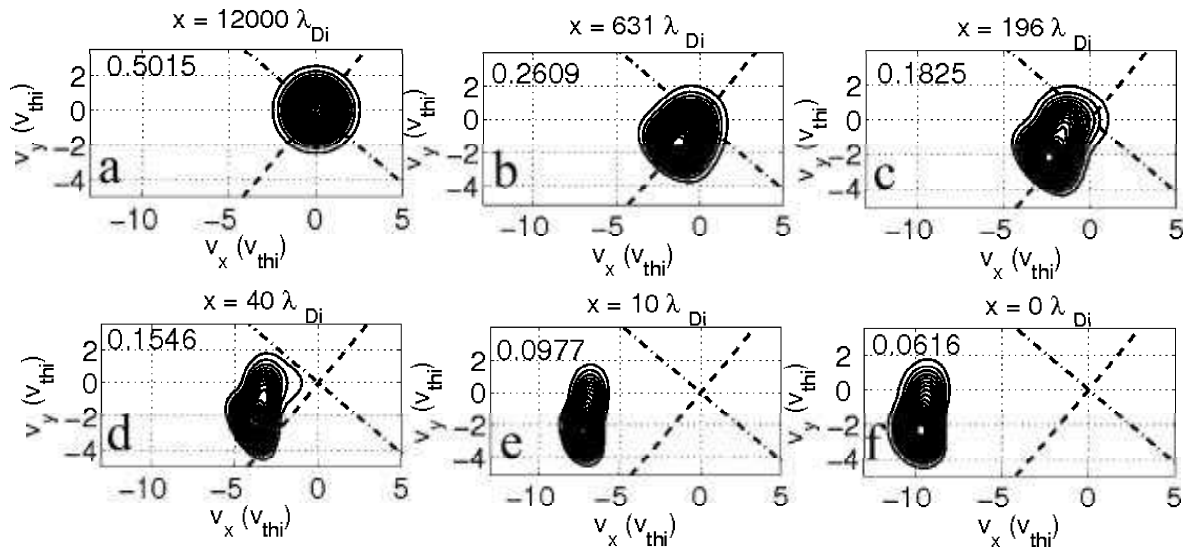


Figure 2: Plasma-wall transition

distribution is here a non-drifting Maxwellian. After leaving the plasma, the ions travel through the first region of the transition, called the collisional presheath (CP). In this region, they are under the combined action of the magnetic field and the collisions, which results in a slow increase of their average velocity along the direction parallel to B (Fig.2b). At around $630\lambda_{Di}$ from the wall (Fig.2c), the ions enter the magnetic presheath (MP): here, the competition is between the magnetic field, which keeps them traveling along the magnetic field lines, and the electric field, which tends to reorient them towards the wall. Following this reorientation, the ions enter the Debye sheath (DS), located at $40\lambda_{Di}$, with a velocity normal to the wall that is close to the sound speed (Fig.2d). Within the Debye sheath, the ions finally undergo a large acceleration towards the wall, due to the large electric field present in the DS (Figs.2e-f).

The ion velocity distribution on the wall is of particular importance for plasma-wall interactions because it can be related to sputtering on the wall. Indeed, the sputtering rate depends of the angle under which the ions hit the wall (here called θ) and on their energy. In Fig.3, we show the velocity distribution in the xOy plane (left part of each plot) and the corresponding angular distribution (right). The distribution displays a large peak with an incidence larger than α and a secondary peak at almost normal incidence. The existence of this two peaks can be explained in terms of the competition between the magnetic field and the effects due to collisions. When the magnetic field is strong compared to the collision rate, the ions are mainly accelerated along the parallel direction, leading to a large peak and a thin tail (Fig. 3c). When the magnetic field is weaker (Fig. 3a-b), the ions are still accelerated along the field lines, but collisions will produce

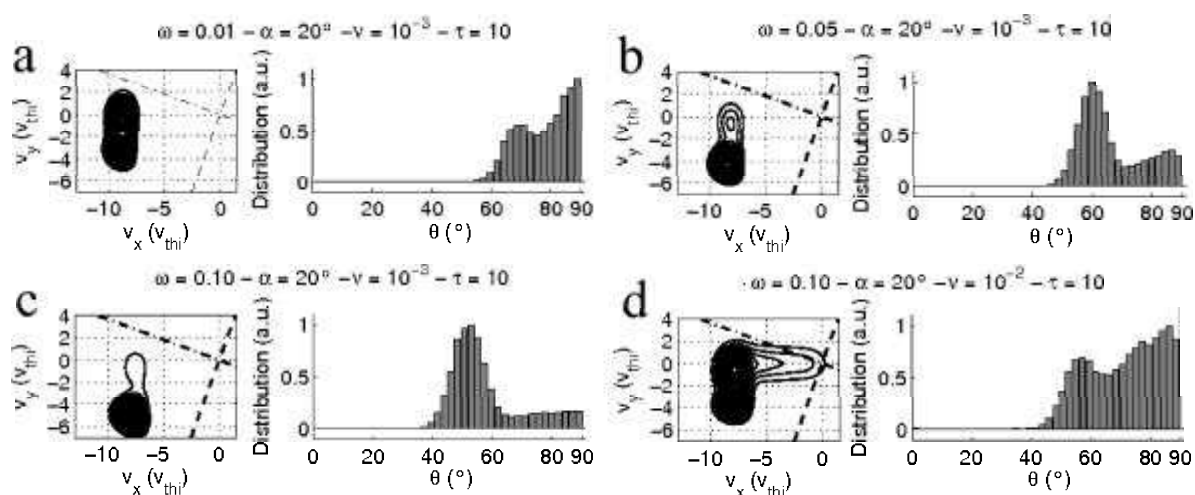


Figure 3: Plasma-wall transition

some ions with small velocity. These ions are then accelerated by the electric field and finally reach the wall at almost normal incidence. The collisional origin of the second ion population is clearly illustrated in Fig. 3d, where the magnetic field strength is the same as in Fig. 3c, but the collision rate is ten times higher: in this case, the distribution is similar to the one observed in the weak B case.

In summary, we have performed numerical simulations of low-pressure argon plasmas in contact with an absorbing wall, with a tilted magnetic field applied. The Eulerian kinetic code used, which takes into account ion-neutral collisions and ionization, allowed us to study the details of the ion distribution along the plasma-wall transition. On the wall, two ion populations have been found. Because of their different velocities and angles of incidence, they may display different behaviors concerning physical adsorption and sputtering at the wall. Further work on this topic will focus on the sputtering rate associated with these two distributions.

References

- [1] F. Valsaque, G. Manfredi, J. P. Gunn, and E. Gauthier, *Phys. Plasmas* **9**, 1806 (2002).
- [2] G. Manfredi and F. Valsaque, *Comp. Phys. Comm.* **164**, 262 (2004).
- [3] R. Chodura, *Phys. Fluids* **25**, 1628 (1982)
- [4] E. Ahedo, *Phys. Plasmas* **4**, 4419 (1997)